Preparation and Characterization of Diorgano- and Dihalogeno-bis(monothio-β-diketonato)tin(IV) Complexes. Crystal and Molecular Structures of $SnY_2(btbm)_2$ and $SnY_2(tacac)_2$ (Y = Me or Cl)†

Channareddy Sreelatha, Dileep K. Srivastava, and Vishnu D. Gupta*
Department of Chemistry, Faculty of Science, Banaras Hindu University, Varanasi 221005, India
Heinrich Nöth*
Institute of Inorganic Chemistry, University of Munich, Meiserstr. 1, D-8000 München, Federal Republic of Germany

Diorgano- and dihalogeno-bis(monothio-β-diketonato)tin(IV) complexes have been prepared and their structures partially deduced by i.r. and n.m.r. data. In order to ascertain structural conclusions, *X*-ray crystal structure analyses were performed on the complexes $SnMe_2(btbm)_2$ [Hbtbm = benzoyl(thiobenzoyl)methane] and $SnMe_2(tacac)_2$ (Htacac = monothioacetylacetone), as well as their dichlorotin(IV) analogues, $SnCl_2(btbm)_2$ and $SnCl_2(tacac)_2$. The tin atoms in $SnMe_2(btbm)_2$ and $SnMe_2(tacac)_2$ show a strongly distorted octahedral environment with pairs of the same donor atoms (O, S) in the *cis* position. The two methyl groups deviate strongly from the *trans* position, C–Sn–C bond angles being 134.2 and 139.4° respectively. Comparatively long Sn–O bond distances reveal the anisobidentate nature of the ligand. In contrast, the dichloro complexes $SnCl_2(btbm)_2$ and $SnCl_2(tacac)_2$ exhibit octahedral geometries, the Cl–Sn–Cl bond angles being only 95.3 and 98.5° respectively, with the chlorine atoms in *cis* positions and the sulphur atoms in *trans* positions. The oxygen atoms show normal Sn–O bond lengths.

Octahedral diorganotin(IV) complexes[1] containing oxygen,[2] nitrogen,[3] and sulphur[4] as donor atoms have been assigned *cis* or *trans* configurations depending on the nature of the ligand and the organo group on tin, as shown by *X*-ray crystallographic studies. In spite of the relative abundance of structural data for six-co-ordinate dimethyltin(IV) compounds, apparently only few data are available for the corresponding dichloro compounds.[5–7] The bonding in tin compounds with co-ordination number six has been described in terms of *d* orbital participation or by invoking the concept of three-centre molecular orbitals, particularly in organotin compounds. In order to gain a better understanding of the stereochemistry of organotin compounds, or even to extend the concept of the Zahrobsky model[8] to chelate structures, asymmetrical sulphur ligand complexes are of special interest. Notably, none of the non-transition metal complexes of asymmetrical organosulphur ligands has been examined so far for structural data, except for our recent report[9] on tris[benzoyl(thiobenzoyl)methanato-*O*,*S*]indium(III). On the other hand several transition-metal bis-,[10,11] tris-,[12] and tetrakis-[13] (monothio-β-diketone) complexes have been examined by *X*-ray structure analysis. In all compounds studied the sulphur atoms of the ligand tend to cluster next to one another irrespective of the geometry of the complex, and normal M–O and M–S distances are observed.

Preliminary studies on $SnMe_2L_2$ complexes (HL = monothio-β-diketone) resulted in two sets of data which led to conflicting interpretations with respect to the arrangement of methyl groups in *cis* or *trans* positions in an octahedral environment. In contrast, non-linearity of the ClSnCl moiety, and, therefore, *cis* geometry in $SnCl_2L_2$ complexes is indicated by infrared spectral studies. In addition, the strength of the bonds between tin and the donor atom (O, S) of the chelating ligand in both complexes remains undefined. In order to settle these points an *X*-ray diffraction study was carried out on $SnY_2(btbm)_2$ and $SnY_2(tacac)_2$ [Hbtbm = benzoyl(thiobenzoyl)methane, Htacac = monothioacetylacetone, Y = Me or Cl].

Experimental

Precautions were taken to exclude moisture. Solvents were dried by standard techniques. Ligands were synthesized by literature procedures.[14,15] The compounds $SnCl_4$ (b.p. 114 °C), $SnMe_2Cl_2$ (b.p. 80 °C, 20 mmHg), $SnBu_2Cl_2$ (b.p. 135 °C, 10 mmHg), and $SnPh_2Cl_2$ (b.p. 100 °C, 0.5 mmHg) were distilled before use. Tin was estimated as SnO_2, and sulphur by Messenger's method. Molecular weights were determined cryoscopically in benzene. I.r. spectra were recorded on a Perkin-Elmer 621 model instrument in the range 4 000—200 cm^{-1} as neat liquids or as Nujol mulls using CsI plates. N.m.r. spectra (^1H, ^{13}C, and ^{119}Sn) were recorded at approximately 25 °C on a JEOL-FX 90 Q spectrometer in $CDCl_3$ or CCl_4 ($SiMe_4$ as internal standard for ^1H and ^{13}C; $SnMe_4$ for ^{119}Sn; sealed capillaries for ^{119}Sn).

General Procedure for the Preparation of Diorgano- and Dihalogeno-bis(monothioacetylacetonato-O,S)tin(IV) *Complexes.*—A stoicheiometric amount of the respective diorganotin(IV) dichloride or tin tetrahalide in dichloromethane (*ca.* 20 cm^3) was added to the sodium salt of monothioacetylacetone[16] suspended in dichloromethane (*ca.* 30 cm^3) with stirring under a nitrogen atmosphere. Stirring was continued for *ca.* 2 h and the sodium chloride formed was removed by filtration. The solvent was then removed *in vacuo* from the filtrate and the products were dried at 28 °C, 0.1 mmHg for 4 h. The products $SnR_2(tacac)_2$ (R = alkyl or aryl) were finally recrystallized from a dichloromethane–n-hexane mixture (1:3) and the dihalogenotin complexes from a chloroform–methanol mixture (1:3). Physical properties and analytical data for the vacuum-dried compounds are given in Table 1.

---

† Bis[benzoyl(thiobenzoyl)methanato-*O*,*S*]dimethyltin(IV), bis[benzoyl(thiobenzoyl)methanato-*O*,*S*]dichlorotin(IV), and dimethyl- and dichloro-(monothioacetylacetonato-*O*,*S*)tin(IV).

Supplementary data available: see Instructions for Authors, *J. Chem. Soc., Dalton Trans.*, 1988, Issue 1, pp. xvii—xx.

Non-S.I. unit employed: mmHg ≈ 133 N m^{-2}.

The complexes $SnMe_2(btbm)_2$ and $SnCl_2(btbm)_2$ were prepared by literature procedures.[17]

X-Ray Structure Analysis.—The *X*-ray structure determinations were performed using a Syntex R3 four-circle automated diffractometer operating with a graphite monochromator and Mo-K_α radiation, λ = 0.710 69 Å, for data collection at 25 °C, and the SHELXTL program [18] for structure solution and refinement. A NOVA 3 computer from Data General was used in all computational work. Crystal data and other details of the *X*-ray crystal structure determinations on $SnY_2(btbm)_2$ and $SnY_2(tacac)_2$ (Y = Me or Cl) are summarized in Table 2.

Table 1. Physical properties of $SnY_2(tacac)_2$ complexes (Y = Me, Bu, Ph, Cl, or I)

Y	Nature	M.p./ °C	Analysis[a]/% Sn	S	$M^{a,b}$
Me	Light yellow solid	92	30.8 (31.3)	16.1 (16.9)	382 (379)
Bu	Light yellow liquid	*c*	25.3 (25.6)	14.0 (13.8)	449 (463)
Ph	Light yellow solid	108	23.1 (23.6)	12.6 (12.7)	531 (520)
Cl	Yellow solid	204	27.8 (28.3)	14.9 (15.2)	402 (419)
I	Yellow solid	178	18.9 (19.6)	11.1 (10.6)	576 (602)

[a] Calculated values in parentheses. [b] Cryoscopically in benzene. [c] Decomposed on attempted distillation.

The yellow crystals of $SnCl_2(btbm)_2$ became opaque in air indicating either slow hydrolysis or the presence of solvent in the crystal lattice. Solvent molecules were detected by density measurement. Refinement of one $CHCl_3$ molecule was difficult, freely refined site-occupation factors favoured the presence of one molecule, but U_{iso} values were still high. Anisotropic refinement indicated disorder, but the split model did not improve results. Therefore, this $CHCl_3$ molecule was refined only isotropically. All H atoms could be observed after anisotropic refinement except that of the isotropically refined $CHCl_3$. Positions and U_{iso} for H(33)—H(35) were not refined in the final stage.

Tables 3—6 contain atomic co-ordinates of the non-hydrogen atoms for $SnMe_2(btbm)_2$, $SnMe_2(tacac)_2$, $SnCl_2(btbm)_2$, and $SnCl_2(tacac)_2$, respectively.

Results and Discussion

The i.r. spectra of monothio-β-diketones[19,20] have been interpreted on the basis of the bands at 1 588—1 602 and 1 555—1 572 cm^{-1} due to $\nu(\mathrm{C}\overset{\cdots}{-}\mathrm{O})$ and $\nu(\mathrm{C}\overset{\cdots}{-}\mathrm{C})$ and at 1 244—1 260 and 820—840 cm^{-1} due to $\nu(\mathrm{C}\overset{\cdots}{-}\mathrm{S})$ and $\nu(\mathrm{C}\overset{\cdots}{-}\mathrm{S})$ + δ(C–H) respectively. The absorption bands observed in $SnR_2(tacac)_2$ (R = Me, Bu, or Ph) complexes (Table 7) at 1 620—1 595 cm^{-1} represent $\nu(\mathrm{C}\overset{\cdots}{-}\mathrm{O})$ and bands at 1 208—1 220 cm^{-1}

Table 2. Crystallographic data[a]

Complex	$SnMe_2(btbm)_2$[b]	$SnMe_2(tacac)_2$[c]	$SnCl_2(btbm)_2{\cdot}2CHCl_3$[d]	$SnCl_2(tacac)_2$[c]
(*a*) Crystal data				
Formula	$C_{32}H_{28}O_2S_2Sn$	$C_{12}H_{20}O_2S_2Sn$	$C_{30}H_{22}Cl_2O_2S_2Sn{\cdot}2CHCl_3$	$C_{10}H_{14}Cl_2O_2S_2Sn$
M	627.38	379.10	906.97	419.91
a/Å	9.864(3)	7.832(1)	11.731(6)	14.688(8)
b/Å	11.013(2)	10.658(5)	12.889(8)	8.145(4)
c/Å	14.418(4)	19.524(5)	14.281(11)	13.939(5)
α/°	109.45(2)	90	98.56(4)	90
β/°	98.89(3)	95.08(4)	114.01(4)	107.66(4)
γ/°	92.26(2)	90	98.65(5)	90
U/Å^3	1 425	1 623	1 897	1 589
D_c/g cm^{-3}	1.435	1.541	1.588	1.756
Z	2	4	2	4
Space group	$P\bar{1}$	$P2_1/c$	$P\bar{1}$	$C2/m$
μ(Mo-K_α)/cm^{-1}	10.45	18.16	13.78	21.94
F(000)	639.54	759.94	899.94	823.95
Size of crystal/mm	0.36 × 0.23 × 0.47	0.3 × 0.28 × 0.4	0.21 × 0.3 × 0.35	0.3 × 0.28 × 0.4
(*b*) Data collection[e]				
2θ range/°	3—50	2—50	2—50	2—50
hkl	$-h\pm k\pm l$	$hk\pm l$	$\pm h\pm k\pm l$	$h\pm k\pm l$
Collected reflections	6 629	2 766	10 742	2 411
Unique reflections, $F \geqslant 3\sigma(F)$	4 357	2 032	5 350	1 230
Max./min. transmission	0.825/0.742	0.941/0.763	0.762/0.672	0.560/0.448
Structure solution	Heavy-atom method	Heavy-atom method	Direct method	Direct method
Final parameters[f]	406	179	463	106
R	0.0397	0.0485	0.0744	0.0314
R′	0.0404	0.0528	0.0781	0.0327
g	0.000 36	0.001 78	0	0.000 57
Largest residual electron density/e Å^{-3}	0.75[g]	0.55[h]	2.0	0.39[i]

[a] Data common to all four determinations: reflection:background ratio = 1:1, scan speed for 150—2 500 counts s^{-1} = 3.3—29.3. [b] By slow evaporation from dichloromethane solution. [c] From dichloromethane–hexane. [d] From chloroform solution by slow evaporation. [e] Two check reflections measured after every 48 intensity measurements by the peak-profile method. Intensities corrected for Lorentz and polarization as well as for absorption effects (empirical, ψ-scan). [f] After refining the structure isotropically and anisotropically, all hydrogen atoms were included with fixed U_{iso} approximated to 1.2 times the U_{eq} value of its carbon atom. [g] Four highest peaks near Sn and S atoms. [h] Disorder of the Me group at C(b) atom indicated by the highest residuals. [i] Highest peaks near Cl atoms.

Table 3. Non-hydrogen atomic co-ordinates (× 10^4) for $SnMe_2(btbm)_2$ with estimated standard deviations (e.s.d.s) in parentheses

Atom	*x*	*y*	*z*
Sn	6 927(1)	2 942(1)	7 593(1)
S(1)	7 581(1)	2 062(1)	8 993(1)
S(2)	7 927(1)	844(1)	6 775(1)
O(1)	6 281(3)	4 680(3)	9 051(2)
O(2)	6 660(4)	2 868(3)	5 829(2)
C(1)	8 015(4)	3 264(4)	10 155(3)
C(2)	7 784(4)	4 551(4)	10 450(3)
C(3)	6 990(4)	5 219(4)	9 904(3)
C(4)	7 545(4)	226(4)	5 473(3)
C(5)	6 939(4)	750(4)	4 816(3)
C(6)	6 511(4)	2 022(4)	4 983(3)
C(7)	4 766(4)	2 643(4)	7 221(3)
C(8)	8 401(5)	4 493(4)	7 780(4)
C(10)	8 713(4)	2 771(4)	10 922(3)
C(11)	9 749(5)	1 956(4)	10 730(4)
C(12)	10 382(6)	1 517(5)	11 477(5)
C(13)	10 014(8)	1 869(5)	12 386(4)
C(14)	8 998(8)	2 667(5)	12 579(4)
C(15)	8 332(6)	3 122(4)	11 865(3)
C(20)	7 006(4)	6 658(4)	10 381(3)
C(21)	8 103(5)	7 409(4)	11 073(3)
C(22)	8 133(6)	8 721(5)	11 452(4)
C(23)	7 059(6)	9 306(4)	11 144(4)
C(24)	5 943(6)	8 591(5)	10 481(4)
C(25)	5 896(5)	7 252(4)	10 075(3)
C(30)	8 000(4)	−1 097(4)	5 068(3)
C(31)	8 744(5)	−1 376(4)	4 293(4)
C(32)	9 169(6)	−2 583(5)	3 913(4)
C(33)	8 887(6)	−3 532(5)	4 291(4)
C(34)	8 162(6)	−3 268(5)	5 058(4)
C(35)	7 710(4)	−2 050(4)	5 450(3)
C(40)	5 850(4)	2 350(4)	4 104(3)
C(41)	5 765(7)	3 633(5)	4 220(4)
C(42)	5 108(9)	3 995(6)	3 450(5)
C(43)	4 534(7)	3 090(7)	2 559(4)
C(44)	4 605(6)	1 802(6)	2 429(4)
C(45)	5 273(5)	1 447(4)	3 191(3)

Table 4. Atomic co-ordinates (× 10^4) for $SnMe_2(tacac)_2$ with e.s.d.s in parentheses

Atom	*x*	*y*	*z*
Sn	2 183(1)	7 662(1)	1 234(1)
S(1)	483(3)	7 084(2)	2 213(1)
C(1)	−973(10)	8 240(7)	2 341(4)
C(2)	−1 653(14)	9 126(9)	1 889(6)
C(3)	−1 479(11)	9 316(7)	1 192(4)
C(4)	−1 612(12)	8 234(9)	3 067(4)
C(5)	−2 420(14)	10 390(10)	836(5)
O(1)	−568(8)	8 639(6)	846(3)
S(2)	4 502(3)	6 437(2)	1 925(1)
C(6)	5 809(10)	5 690(7)	1 384(4)
C(7)	6 133(11)	5 993(8)	729(4)
C(8)	5 617(10)	7 083(7)	332(4)
O(2)	4 631(8)	7 886(5)	503(3)
C(9)	6 450(14)	7 246(8)	−333(4)
C(10)	6 697(13)	4 556(8)	1 715(5)
C(a)	2 873(13)	9 595(7)	1 374(4)
C(b)	1 293(12)	6 407(8)	427(4)

Table 5. Atomic co-ordinates (× 10^4) for $SnCl_2(btbm)_2$ with e.s.d.s in parentheses

Atom	*x*	*y*	*z*
Sn(1)	108(1)	7 516(1)	2 662(1)
Cl(1)	1 688(2)	8 308(2)	4 456(2)
Cl(2)	218(3)	5 680(2)	2 762(2)
S(1)	1 761(2)	7 947(2)	2 042(2)
C(2)	1 234(8)	7 083(7)	826(7)
C(3)	49(8)	6 451(7)	199(7)
C(4)	−1 124(9)	6 418(7)	261(7)
O(5)	−1 208(6)	6 968(5)	1 049(5)
C(6)	2 242(9)	7 132(7)	428(7)
C(7)	3 545(10)	7 396(8)	1 119(8)
C(8)	4 462(11)	7 456(10)	728(10)
C(9)	4 095(12)	7 284(11)	−323(10)
C(10)	2 806(12)	7 037(13)	−1 024(9)
C(11)	1 899(10)	6 955(10)	−635(8)
C(12)	−2 354(8)	5 789(7)	−615(7)
C(13)	−2 455(10)	5 258(8)	−1 572(7)
C(14)	−3 631(11)	4 701(10)	−2 380(8)
C(15)	−4 735(10)	4 679(10)	−2 238(9)
C(16)	−4 652(11)	5 183(11)	−1 281(10)
C(17)	−3 476(11)	5 752(10)	−486(9)
S(20)	−1 826(2)	7 285(2)	2 966(2)
C(21)	−1 905(8)	8 564(7)	3 480(6)
C(22)	−1 241(9)	9 536(7)	3 530(7)
C(23)	−439(8)	9 800(7)	3 032(6)
O(24)	−141(6)	9 085(5)	2 501(5)
C(25)	−2 920(8)	8 515(7)	3 866(6)
C(26)	−3 733(10)	9 220(8)	3 635(8)
C(27)	−4 708(11)	9 153(11)	3 951(10)
C(28)	−4 834(11)	8 414(12)	4 523(11)
C(29)	−4 045(11)	7 705(10)	4 764(9)
C(30)	−3 090(9)	7 757(9)	4 432(8)
C(31)	74(9)	10 943(7)	3 061(7)
C(32)	−293(10)	11 809(8)	3 476(8)
C(33)	193(13)	12 824(9)	3 468(10)
C(34)	1 104(13)	13 037(9)	3 091(10)
C(35)	1 447(13)	12 187(10)	2 669(10)
C(36)	960(11)	11 159(8)	2 664(9)
C(40)	2 823(12)	6 159(10)	5 613(9)
Cl(41)	1 913(4)	5 277(3)	6 018(3)
Cl(42)	3 675(4)	5 401(4)	5 104(3)
Cl(43)	3 864(5)	7 203(3)	6 661(3)
C(50)	2 802(36)	−155(30)	164(30)
Cl(51)	3 171(8)	249(7)	−693(7)
Cl(52)	3 885(10)	634(8)	1 531(8)
Cl(53)	1 429(13)	267(11)	103(11)

Table 6. Atomic co-ordinates (× 10^4) for $SnCl_2(tacac)_2$ with e.s.d.s in parentheses

Atom	*x*	*y*	*z*
Sn	0 000	2 092(1)	2 500
S	−386(1)	2 276(2)	4 090(1)
C(1)	617(4)	3 045(6)	4 975(4)
C(2)	1 365(4)	3 864(7)	4 816(4)
C(3)	1 506(3)	4 414(6)	3 915(4)
C(4)	2 322(6)	5 575(11)	3 990(7)
C(5)	578(6)	2 797(10)	6 031(5)
O	988(2)	4 076(4)	3 036(2)
Cl	1 292(1)	155(2)	3 112(1)

result from ν(C⋯S). The position of the ν(C⋯O) band is intermediate between free[21,22] and chelated carbonyl[19,20] absorptions indicating asymmetrical or anisobidentate[23] co-ordination of the ligand tacac. The diagnostic spectral bands are very similar to those reported[17] for $SnR_2(btbm)_2$ (R = Me, Bu, or Ph). Thus, $SnR_2(tacac)_2$ may exist as a tetrahedral tin species, with very little interaction between the tin atom and oxygen atoms, or as a six-co-ordinate species with weak Sn–O bonding.

In the far-i.r. region, all the bis complexes exhibit medium to strong bands at 472—492 and 368—377 cm^{-1}, assignable to ν(Sn–O)[24] and ν(Sn–S)[25] vibrations respectively. A band at 567 cm^{-1} is assignable to $\nu_{asym}(SnC_2)$[26] and no band due to

Table 7. Selected and typical i.r. bands (cm^{-1}) for SnY$_2$(tacac)$_2$ complexes[a]

Y	ν(C–O)	ν(C–C)	ν(C–S)	ν(C–S) + δ(C–H)	ν(Sn–C)	ν(Sn–O)	ν(Sn–S)	ν(Sn–Y)
Me	1 620s	1 505s	1 208vs	827m	567s	487m	377s	
Bu	1 620s	1 505s	1 210vs	829m	569s	482m	368s	
Ph	1 595s	1 510s	1 220vs	827w	287m 235m	472m	374s	
Cl	1 567s	*b*	1 240vs	830w		492sm	370s	310m 295m
I	1 563s	*b*	1 235vs	828m		492m	375s	

[a] s = Strong, vs = very strong, m = medium, sm = strong medium, w = weak. [b] Coupled with Nujol band.

Table 8. Hydrogen-1, ^{13}C, and ^{119}Sn chemical shifts[a]

SnMe$_2$(tacac)$_2$[b]	SnBu$_2$(tacac)$_2$	SnPh$_2$(tacac)$_2$	SnMe$_2$(btbm)$_2$	SnCl$_2$(tacac)$_2$	SnI$_2$(tacac)$_2$	Assignments
^{1}H N.m.r.[c]						
2.05	*d*	1.85	*d*	2.29	2.24	CH$_3$–(O)
2.22		2.18		2.40	2.31	CH$_3$–(S)
6.27		5.98		6.51	6.60	>CH–
0.88						CH$_3$–Sn
		6.91—8.14 (multiplet)				Ph–Sn
^{13}C[e]						
192.7	196.1	*f*	189.5	194.7	199.4	>C–(S)
171.5	171.7		174.1	181.7	183.6	>C–(O)
119.2	119.2		117.6	104.9	106.7	>CH–
33.8	35.5			33.6	32.4	CH$_3$–(S)
31.3	30.2			30.4	30.6	CH$_3$–(O)
9.77			9.04			CH$_3$–Sn
	28.3					α–C Bu–Sn
	28.0					β–C Bu–Sn
	26.0					γ–C Bu–Sn
	13.7					δ–C Bu–Sn
		g	*g*			
^{119}Sn[h]						
−220	−230	−253	−220	−266	−263	

[a] At 90 MHz. [b] $^2J(^{119}Sn-^1H) = 88$ and $^1J(^{119}Sn-^{13}C) = 724$ Hz. [c] In CCl$_4$ with SiMe$_4$ as internal reference. [d] Data reported in ref. 17. [e] In CDCl$_3$ with SiMe$_4$ as internal reference. [f] Could not be recorded due to poor solubility. [g] Data on phenyl carbons omitted for brevity. [h] In CDCl$_3$ with SnMe$_4$ as a reference in sealed capillaries.

ν_{sym}(SnC$_2$) is observed in the i.r. spectrum of SnMe$_2$(tacac)$_2$ (Table 7). This indicates that the six-co-ordinate situation, with a *trans* arrangement of the methyl groups, seems to be a good description of the geometry at the tin atom in this molecule. Tin-119 Mössbauer spectra[17] of SnMe$_2$L$_2$ (L = btbm or tacac) gave quadrupole splitting values in a narrow range. On the basis of the recent correlation[27] of the quadrupole splitting with the C–Sn–C bond angles in octahedral complexes, Saini *et al.*[17] deduced distorted structures for these complexes. In contrast, the two i.r. bands observed at 287 and 235 cm^{-1} for SnPh$_2$(tacac)$_2$, which we assign[26,27] to ν_{asym}(SnC$_2$) and ν_{sym}(SnC$_2$) modes respectively, not only indicate six-co-ordination at tin but also *cis* positions for the aryl groups. It can therefore be concluded from the i.r. data that SnMe$_2$(tacac)$_2$ differs considerably in its structure from SnPh$_2$(tacac)$_2$, although no definite configuration can be suggested.

The ^{1}H n.m.r. spectra of SnR$_2$(tacac)$_2$ (R = Me, Bu, or Ph) compounds exhibit three signals (Table 8) corresponding to methine, thioacetyl, and acetyl protons. An additional singlet or multiplet is observed for the protons of the methyl or phenyl groups attached to the tin atom. The value of the observed coupling constant $^2J(^{119}Sn-Me)$ is *ca.* 88 Hz for SnMe$_2$(tacac)$_2$ which is characteristic of six-co-ordinate tin and lies between the reported values for octahedral SnMe$_2$(quin)$_2$[28] (quin = quinolin-8-olate) and SnMe$_2$(acac)$_2$[24] (Hacac = acetylacetone) complexes having *cis* and *trans* configurations respectively. Carbon-13 n.m.r. spectra of SnR$_2$(tacac)$_2$ (R = Me or Bu) are not useful in discriminating further, since they exhibit only one set of resonances for ligand carbons, one for methyl, and four for butyl carbons (Table 8).

The magnitude of $J(^{119}Sn-^{13}C)$ coupling constants[29] of organotin(IV) compounds reflects the hybridization state. The value $^1J(^{119}Sn-^{13}C) = 724$ Hz for SnMe$_2$(tacac)$_2$ falls in the region for six-co-ordinate tin. This comparatively low magnitude with respect to regular *trans* octahedral dialkylbis(β-diketonato)tin(IV) complexes (901—966 Hz)[29,30] may be indicative of substantial distortion of C–Sn–C bonds from the *trans* orientation. The low value of 552 Hz reported for SnEt$_2$[SC(O)NMe$_2$]$_2$[31] is, therefore, rather surprising.

Tin-119 chemical shifts (−220 to −266 p.p.m.) of a few bis(monothio-β-diketonates) are summarized in Table 8. The high-field signals are fully consistent with a six-co-ordinate structure in solution. The somewhat higher value for the diphenyltin complex in comparison to the other dialkyltin compounds may be accounted for in terms of increased polarizability[32,33] of the phenyl groups or structural changes, since the data are close to those of dichlorotin complexes which have been found to be *cis* octahedral. The values of δ observed are low-field with respect to those reported for SnMe$_2$L$'_2$ (L$'$ = β-diketonate or dithiocarbamate; *ca.* 356[34,35] or *ca.* 335 p.p.m.,[35,36] respectively) but are comparable to dialkylbis(quinolin-8-olato)tin(IV) complexes (*ca.* 235 p.p.m.).[35,37,38] Consequently, the n.m.r. data

Table 9. Selected bond distances (Å) and angles (°) for $SnY_2(btbm)_2$ and $SnY_2(tacac)_2$ (Y = Me or Cl)

$SnMe_2(btbm)_2$		$SnMe_2(tacac)_2$		$SnCl_2(btbm)_2$		$SnCl_2(tacac)_2$	
Sn–S(1)	2.526(2)	Sn–S(1)	2.502(2)	Sn–Cl(1)	2.414(2)	Sn–Cl	2.416(1)
Sn–S(2)	2.535(2)	Sn–S(2)	2.528(2)	Sn–Cl(2)	2.410(3)	Sn–S	2.453(2)
Sn–O(1)	2.514(3)	Sn–O(1)	2.452(6)	Sn–S(1)	2.464(3)	Sn–O	2.149(3)
Sn–O(2)	2.489(3)	Sn–O(2)	2.501(7)	Sn–S(20)	2.462(4)	S–C(1)	1.728(5)
Sn–C(7)	2.101(4)	Sn–C(a)	2.142(8)	Sn–O(5)	2.117(9)	C(1)–C(2)	1.360(8)
Sn–C(8)	2.117(5)	Sn–C(b)	2.136(8)	Sn–O(24)	2.120(7)	C(2)–C(3)	1.407(8)
S(1)–C(1)	1.731(3)	S(1)–C(1)	1.711(8)	S(1)–C(2)	1.727(9)	O–C(3)	1.261(6)
S(2)–C(4)	1.743(4)	S(2)–C(6)	1.728(8)	S(20)–C(21)	1.734(10)	C(3)–C(4)	1.505(10)
O(1)–C(3)	1.252(4)	O(1)–C(3)	1.254(10)	O(5)–C(4)	1.285(12)	C(1)–C(5)	1.504(10)
O(2)–C(6)	1.247(4)	O(2)–C(8)	1.218(10)	O(24)–C(23)	1.285(12)		
C(1)–C(2)	1.377(6)	C(1)–C(2)	1.368(12)	C(2)–C(3)	1.352(11)		
C(2)–C(3)	1.419(6)	C(2)–C(3)	1.395(14)	C(3)–C(4)	1.409(16)		
C(4)–C(5)	1.344(6)	C(6)–C(7)	1.366(11)	C(21)–C(22)	1.347(13)		
C(5)–C(6)	1.432(6)	C(7)–C(8)	1.435(11)	C(22)–C(23)	1.424(16)		

$SnMe_2(btbm)_2$		$SnMe_2(tacac)_2$		$SnCl_2(btbm)_2$		$SnCl_2(tacac)_2$	
S(1)–C(1)–C(2)	130.0(3)	S(1)–C(1)–C(2)	129.0(7)	S(1)–Sn–S(20)	166.8(1)	S(A)–Sn–S	173.0(1)
S(2)–C(4)–C(5)	130.5(3)	S(2)–C(6)–C(7)	129.2(6)	O(5)–Sn–O(24)	86.9(2)	O(A)–Sn–O	82.5(2)
O(1)–C(3)–C(2)	123.9(4)	O(1)–C(3)–C(2)	123.5(7)	Cl(1)–Sn–Cl(2)	95.3(1)	Cl(A)–Sn–Cl	98.5(1)
O(2)–C(6)–C(5)	123.1(4)	O(2)–C(8)–C(7)	125.1(7)	S(1)–Sn–O(5)	86.2(2)	O–Sn–S	87.5(1)
C(1)–C(2)–C(3)	128.9(3)	C(1)–C(2)–C(3)	131.6(9)	S(20)–Sn–O(5)	84.6(2)	O(A)–Sn–S	87.2(1)
C(4)–C(5)–C(6)	129.8(3)	C(6)–C(7)–C(8)	129.1(8)	S(1)–Sn–O(24)	83.9(2)	Cl–Sn–O	89.6(1)
S(1)–Sn–S(2)	75.8(1)	S(1)–Sn–S(2)	82.6(1)	S(20)–Sn–O(24)	86.3(2)	S–Sn–Cl	95.3(0)
O(1)–Sn–O(2)	127.4(1)	O(1)–Sn–O(2)	118.7(2)	S(1)–Sn–Cl(1)	89.9(1)	O(A)–Sn–Cl	171.6(1)
C(7)–Sn–C(8)	134.2(2)	C(a)–Sn–C(b)	139.4(3)	S(20)–Sn–Cl(1)	98.5(1)	Cl(A)–Sn–S	89.2(0)
S(1)–Sn–O(1)	78.3(1)	S(1)–Sn–O(1)	80.1(1)	S(1)–Sn–Cl(2)	98.7(1)	Sn–S–C(1)	106.6(2)
S(2)–Sn–O(1)	154.1(1)	S(2)–Sn–O(1)	162.7(1)	S(20)–Sn–Cl(2)	90.6(1)	Sn–O–C(3)	130.3(3)
S(2)–Sn–O(2)	78.5(1)	S(2)–Sn–O(2)	78.6(1)	O(5)–Sn–Cl(1)	174.0(2)	S–C(1)–C(2)	128.2(4)
S(1)–Sn–O(2)	154.2(1)	S(1)–Sn–O(2)	161.1(1)	O(24)–Sn–Cl(1)	88.2(2)	O–C(3)–C(2)	126.2(5)
S(1)–Sn–O(7)	105.8(2)	S(1)–Sn–C(b)	104.4(2)	O(5)–Sn–Cl(2)	89.8(2)	C(1)–C(2)–C(3)	130.2(5)
S(2)–Sn–C(7)	109.0(1)	S(2)–Sn–C(b)	104.0(2)	O(24)–Sn–Cl(2)	175.6(2)		
S(1)–Sn–C(8)	108.6(2)	S(1)–Sn–C(a)	106.5(2)	Sn–S(1)–C(2)	107.0(4)		
S(2)–Sn–C(8)	108.0(1)	S(2)–Sn–C(a)	105.5(2)	Sn–S(20)–C(21)	106.6(3)		
O(1)–Sn–C(7)	79.5(1)	O(1)–Sn–C(a)	80.5(3)	Sn–O(5)–C(4)	131.7(6)		
O(2)–Sn–C(7)	81.3(2)	O(2)–Sn–C(a)	77.5(3)	Sn–O(24)–C(23)	131.3(7)		
O(1)–Sn–C(8)	78.9(2)	O(1)–Sn–C(b)	79.5(3)	S(1)–C(2)–C(3)	128.3(9)		
O(2)–Sn–C(8)	80.7(2)	O(2)–Sn–C(b)	81.7(3)	S(20)–C(21)–C(22)	129.4(9)		
Sn–S(1)–C(1)	113.0(2)	Sn–S(1)–C(1)	109.9(3)	O(5)–C(4)–C(3)	122.8(7)		
Sn–S(2)–C(4)	115.7(1)	Sn–S(2)–C(6)	110.4(3)	O(24)–C(23)–C(22)	123.1(8)		
Sn–O(1)–C(3)	127.8(3)	Sn–O(1)–C(3)	127.2(5)	C(2)–C(3)–C(4)	130.8(9)		
Sn–O(2)–C(6)	137.2(3)	Sn–O(2)–C(8)	128.8(5)	C(21)–C(22)–C(23)	129.5(9)		

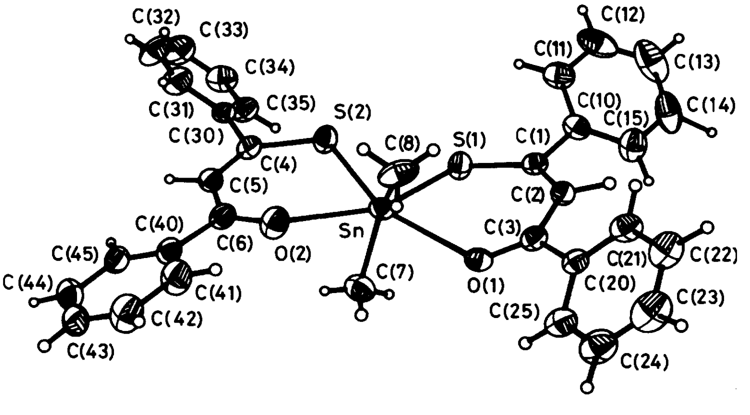

Figure 1. ORTEP plot of molecular structure of $SnMe_2(btbm)_2$. Thermal ellipsoids represent a 30% probability level

are of little help in deriving an unambiguous structural assignment for $SnR_2(tacac)_2$.

I.r. spectra of $SnX_2(tacac)_2$ (X = Cl or I, see Table 7) show bands in the 1 565(±2) cm^{-1} region, assigned to $\nu(\mathrm{C}\overset{\cdots}{-}\mathrm{O})$. These are at lower frequency than those found in $SnMe_2(tacac)_2$, suggesting Sn–O bonding and, therefore, a bidentate mode of attachment of the ligand moiety. In addition, two clearly

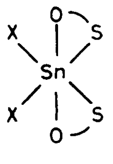

(I)

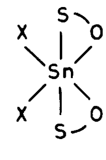

(II)

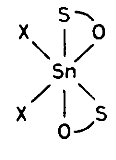

(III)

Table 10. Dimensions of $SnO_2S_2C_2$, SnS_4C_2, and SnO_4C_2 cores; distances in Å, angles in °

Complex	Sn–O	Sn–S	Sn–C or Sn–Cl	C–Sn–C or Cl–Sn–Cl	Ref.
$SnMe_2(btbm)_2$	2.514	2.526	2.101	134.2	This work
	2.489	2.535	2.117		
$SnMe_2(tacac)_2$	2.452	2.502	2.142	139.4	This work
	2.501	2.528	2.136		
$SnMe_2(dtc)_2$		2.515		136.0	4
		2.497[a]	2.16		
		2.954			
		3.061[b]	2.13		
$SnMe_2(acac)_2$	2.20		2.14	180.0	2
	2.18				
$SnCl_2(btbm)_2$	2.117	2.464	2.414	95.3	This work
	2.120	2.462	2.410		
$SnCl_2(tacac)_2$	2.149	2.453	2.416	98.5	This work
$SnCl_2(acac)_2$	2.058		2.354	96.8	6

[a] Single bond distance. [b] Longer bond length.

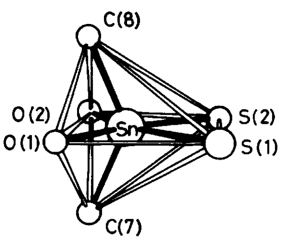

Figure 2. Plot of the distorted octahedral arrangement of atoms bound directly to tin in $SnMe_2(btbm)_2$. Contour lines do not represent chemical bonds

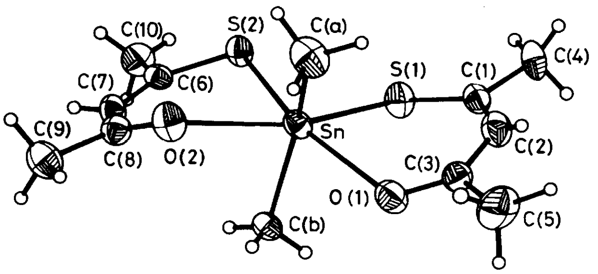

Figure 3. ORTEP plot of the molecular structure of $SnMe_2(tacac)_2$. Thermal ellipsoids represent a 30% probability level

resolved bands at 310 and 295 cm^{-1} due to $\nu_{asym}(SnCl_2)$ and $\nu_{sym}(SnCl_2)$ modes[39] were observed indicating non-linearity of the ClSnCl group and suggesting a *cis*-$SnCl_2L_2$ arrangement. This information, along with the ^{13}C n.m.r. data, which exhibit a single set of resonances for the ligands in $SnCl_2(tacac)_2$ and $SnI_2(tacac)_2$, and ^{119}Sn chemical shifts (Table 8) does not allow one to distinguish between the geometrical isomers (**I**)—(**III**). Therefore, the crystal structures of $SnCl_2(btbm)_2$, $SnCl_2(tacac)_2$, $SnMe_2(tacac)_2$, and $SnMe_2(btbm)_2$ were determined to provide unequivocal evidence of the configurations of these two classes of compound.

Crystal and Molecular Structures.—The molecular structures of $SnMe_2(btbm)_2$ and $SnMe_2(tacac)_2$ shown in Figures 1—3 are essentially similar, differing only in crystalline environments. Due to the greater propensity of β-diketones for chelation, the molecules contain a six-co-ordinate tin atom and the most important feature of the geometry at tin is that pairs of donor atoms of the same type are found next to one another (Figure 2). Data in Table 9 reveal that the bond distances to comparable atoms are almost identical and can be considered as equal by the 3σ criterion.

Although the sulphur atom has a much larger atomic radius than oxygen, the mean Sn–O bond distance in $SnMe_2(btbm)_2$ and $SnMe_2(tacac)_2$ (Sn–O, 2.501 and 2.475 Å respectively) is almost as long as the mean Sn–S distance (Sn–S, 2.530 and 2.515 Å respectively). The Sn–S bond length falls into the normal range for six-co-ordinate tin (2.49—2.67 Å)[4] and is comparable to the Sn–S single bond distance in the dithiocarbamate (dtc) analogue.[4] These are slightly longer than the sum (2.44 Å) of the covalent radii of tin and sulphur.[40] Dimensions of $SnO_2S_2C_2$, SnS_4C_2, and SnO_4C_2 cores in $SnX_2L'_2$ [X = Me or Cl, L′ = btbm, tacac, acac, or dtc) complexes are given in Table 10 for comparison.

The Sn–O bond usually falls in the range 2.11—2.45 Å for octahedral tin complexes,[1] but the Sn–O bond lengths in $SnMe_2(btbm)_2$ and $SnMe_2(tacac)_2$ are much longer than the 2.19 Å reported for $SnMe_2(acac)_2$[2] indicating weakly co-ordinated oxygen atoms. They are comparable with the Sn–O bond (2.520 Å) found in $SnCl_2(CH_2CH_2COOMe)_2$, a compound thought to contain a six-co-ordinate tin atom.[41] In fact, the Sn–O distances determined in dimethyltin complexes exceed the sum of the covalent radii (2.11 Å) of tin and oxygen[40] by *ca.* 18%. Thus, these bis(monothio-β-diketonates) are the first examples of a metal complex where the ligand is found to exhibit an *anisobidentate* nature with weak Sn–O bonds compared to the Sn–S bonds. In monothio-β-diketonates of transition metals[10–13] the metal to oxygen or sulphur bonds correspond to the sum of the covalent radii.

The result described above has a contrasting mode of bonding to the diphenyltin(IV) complex $[SnPh_2(OH)Sn\{OP(S)(OPh)_2\}]_2$.[42] The ligand is only bound by oxygen to the tin atom at the centre of a highly distorted trigonal-bipyramidal environment; the sulphur atom is not in the bonding range, intra- or inter-molecularly. Furthermore, in similar systems containing the ligand $(RCH_2O)_2PSO^-$, spectroscopic evidence[43] for triorganotin complexes suggests a preference for Sn–O rather than Sn–S covalent bond formation. The difference in the behaviour of organo-sulphur ligands and asymmetrical sulphur phosphate esters towards the organotin moiety is surprising. Spectroscopic results from triorgano(monothio-β-diketonato)tin(IV) complexes[44] and *X*-ray crystal data on a series of organotin(IV) monothiocarbamates[45] strongly suggest

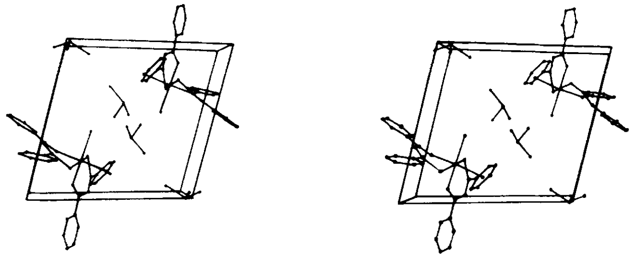

Figure 4. Packing diagram for SnCl$_2$(btbm)$_2$ viewed down the *a* axis. Hydrogen atoms are omitted; CHCl$_3$ molecules are arranged along the [011] plane

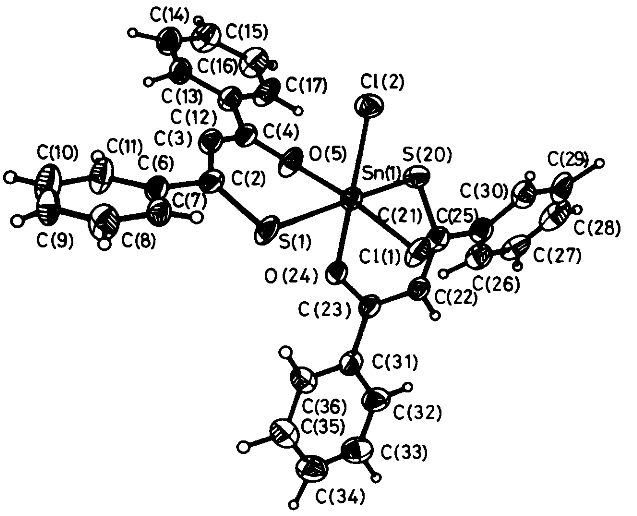

Figure 5. ORTEP plot of the molecular structure of SnCl$_2$(btbm)$_2$. Thermal ellipsoids represent a 30% probability level

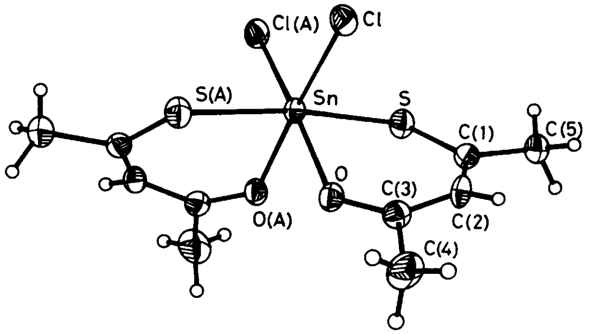

Figure 6. ORTEP plot of the molecular structure of SnCl$_2$(tacac)$_2$. Thermal ellipsoids represent a 30% probability level

preferential affinity of the organotin moiety to bind to sulphur in such systems.

The Sn–C(Me) bond lengths in SnMe$_2$L$_2$ (L = btbm or tacac) complexes are in good agreement with reported values[2–4] and correspond well with the sum of covalent radii (2.14 Å) of carbon and tin.[40] The most interesting feature for these complexes is that the C–Sn–C bond angles [134.2 and 139.4° respectively for SnMe$_2$(btbm)$_2$ and SnMe$_2$(tacac)$_2$] deviate considerably from 90°, expected for a *cis* octahedral complex, but also from a *trans* octahedral geometry, where the ideal C–Sn–C bond angle would be 180°. Moreover, this angle is not compatible with a tetrahedral arrangement. The interligand O–Sn–O bond angles, averaging 123°, are in contrast to the acute S–Sn–S angles (75.8 and 82.6° respectively). As expected, the O–Sn–S bond angles are smaller than 90°; this follows from the geometry of the chelate ring where all angles of the six-membered ring exceed 120°, except at the tin and sulphur atoms. A comparison of the bond angles in the two chelate rings in SnMe$_2$(btbm)$_2$ reveals that they compare favourably except at the oxygen atoms where they differ by almost 10°. The reason for this deviation cannot be readily explained because bond lengths compare well for the two six-membered rings.

The packing diagram for SnCl$_2$(btbm)$_2$ and the molecular structures of SnCl$_2$(btbm)$_2$ and SnCl$_2$(tacac)$_2$ are shown in Figures 4—6. The molecules contain a six-co-ordinate tin atom and a geometry approaching a regular octahedron, in contrast to the highly distorted octahedral structure of SnMe$_2$ complexes. Data in Table 9 contain selected bond lengths and bond angles. However, details of the structure of the two dichlorotin(IV) compounds differ slightly but significantly. Thus, SnCl$_2$(tacac)$_2$ possesses true C_2 symmetry due to a crystallographic two-fold axis, in contrast to SnCl$_2$(btbm)$_2$. Notably, the Cl atoms in SnCl$_2$(btbm)$_2$ and SnCl$_2$(tacac)$_2$ adopt a *cis* orientation with Cl–Sn–Cl bond angles of 95.3 and 98.5° respectively, similar to the analogous compound SnCl$_2$(acac)$_2$[6] (96.8°). The other most important feature is the *trans* orientation of the two sulphur atoms, the S–Sn–S bond angles being 166.8 and 173.0° for SnCl$_2$(btbm)$_2$ and SnCl$_2$(tacac)$_2$ respectively.

Some significant comparison can be made between the dichloro and the dimethyl compounds with regard to Sn–S and Sn–O bond distances (Table 10). In the chloro complexes both these distances approach the sum of the covalent radii, revealing a much stronger Sn–O interaction as well as a slightly stronger Sn–S bond, and, therefore, a bidentate behaviour of the monothio-β-diketonate ligand. Consequently, the ligating properties of the monothio-β-diketones are obviously determined by the Lewis-acid behaviour of the SnY$_2$ unit, which is not unexpected in terms of the electronegativity difference between the chlorine atom and the methyl group. This is also reflected in the larger intra-chelate angles (*ca.* 87°) subtended at tin in the dichloro compounds in comparison with the dimethyltin(IV) complexes (*ca.* 78°). A comparison (Table 10) of tin–ligand bonds between regular *cis* octahedral SnCl$_2$L$_2$ and the analogous SnCl$_2$(acac)$_2$ complex shows that in the latter both Sn–Cl and Sn–O bond distances are much shorter, showing that acac is strongly chelated to the tin atom.

The intra-chelate angles merit some comment. All the angles subtended at carbon atoms are found in the range of 123—132°, exceeding the ideal 120°, indicating some opening of the angles after chelation. The co-ordination asymmetry results in Sn–S–C and Sn–O–C angles in the ranges of 107—116 and 127—137° respectively which may be compared with the corresponding angles (110.8 and 133.8°) in [Ni(tacac)$_2$],[10] [Co(dtacac)$_2$][46] (Co–S–C 118°; dtacac = dithioacetylacetonate), and SnCl$_2$(acac)$_2$ (Sn–O–C 125°).[6] In the case of [Zr(tacac)$_4$],[13] the angle at oxygen opens further to 145°. In fact, the Zr–O bond appears to be shortened at the expense of the Zr–S bond.

The observed interatomic distances in the chelate rings are

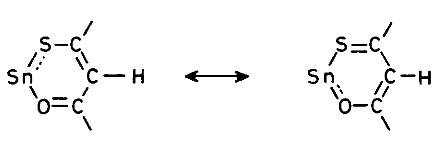

(A) **(B)**

consistent with delocalization of the π-bond frame. However, it is interesting that the C–C bond adjacent to the C–S bond is slightly shorter than the C–C bond adjacent to the C–O group. This feature compares favourably with C–O bond lengths found in carboxylates, suggesting that the resonance form (**A**) contributes more to the ground state than (**B**). The substituents on the pseudo-aromatic ring do not effect the configuration of the bis(monothio-β-diketonato)tin(IV) complexes. On the contrary,[47] in dithiophosphates, $SnPh_2[SP(S)(OR)_2]_2$ the C–Sn–C angle opens from 135° in the case of diethyl phosphate (R = Et) to *ca.* 180° in the di-isopropyl phosphate ($R = Pr^i$), and the ligand loses its asymmetrical mode of bonding in the latter case.

Acknowledgements

Miss Ch. Sreelatha and Mr. D. K. Srivastava are grateful to C.S.I.R., New Delhi (India) for the award of SRF. The assistance of Dr. W. Rattay in the structure determination is gratefully acknowledged.

References

1 J. A. Zubieta and J. J. Zuckerman, *Prog. Inorg. Chem.*, 1978, **24**, 251.
2 G. A. Miller and E. O. Schlemper, *Inorg. Chem.*, 1973, **12**, 677.
3 E. O. Schlemper, *Inorg. Chem.*, 1967, **6**, 2012.
4 T. Kimura, N. Yasuoka, N. Kasai, and M. Kakudo, *Bull. Chem. Soc. Jpn.*, 1972, **45**, 1649; J. S. Morris and E. O. Schlemper, *J. Cryst. Mol. Struct.*, 1979, **9**, 13.
5 P. G. Harrison, T. J. King, and J. A. Richards, *J. Chem. Soc., Dalton Trans.*, 1976, 1414.
6 G. A. Miller and E. O. Schlemper, *Inorg. Chim. Acta*, 1978, **30**, 131.
7 S. W. Cowan, R. W. Gable, B. F. Hoskins, and G. Winter, *Inorg. Chim. Acta*, 1983, **77**, L 225.
8 R. F. Zahrobsky, *J. Am. Chem. Soc.*, 1971, **93**, 3313.
9 Ch. Sreelatha, V. D. Gupta, C. K. Narula, and H. Nöth, *J. Chem. Soc., Dalton Trans.*, 1985, 2623.
10 O. Siiman, D. D. Titus, C. D. Cowman, J. Fresco, and H. B. Gray, *J. Am. Chem. Soc.*, 1974, **96**, 2353.
11 J. Coetzler and J. C. A. Boyens, *J. Cryst. Mol. Struct.*, 1971, **1**, 277.
12 B. F. Hoskins and C. D. Pannan, *Inorg. Nucl. Chem. Lett.*, 1975, **11**, 409.
13 M. E. Silver, H. K. Chun, and R. C. Fay, *Inorg. Chem.*, 1982, **21**, 3765.
14 E. Uhlemann and H. Müller, *Angew. Chem., Int. Ed. Engl.*, 1965, **4**, 154.
15 F. Duus and J. W. Anthonsen, *Acta Chem. Scand., Ser. B*, 1977, **31**, 40.
16 O. Siiman and J. Fresco, *J. Chem. Phys.*, 1971, **54**, 734.
17 S. K. Saini, V. D. Gupta, R. C. Mehrotra, and R. P. Tripathi, *Aust. J. Chem.*, 1980, **33**, 1137.
18 G. M. Sheldrick, SHELXTL, program for crystal structure determination, Göttingen, 1983.
19 S. E. Livingstone, *Coord. Chem. Rev.*, 1971, **7**, 59.
20 M. Cox and J. Darken, *Coord. Chem. Rev.*, 1971, **7**, 29.
21 S. H. H. Chaston and S. E. Livingstone, *Aust. J. Chem.*, 1967, **20**, 1079.
22 F. Duus, *J. Org. Chem.*, 1977, **42**, 3123.
23 J. L. K. F. deVries and R. H. Herber, *Inorg. Chem.*, 1972, **11**, 2458.
24 M. M. McGrady and R. S. Tobias, *J. Am. Chem. Soc.*, 1965, **87**, 1909.
25 D. C. Bradley and M. H. Gitlitz, *J. Chem. Soc. A*, 1969, 1152.
26 M. K. Das, M. Nath, and J. J. Zuckerman, *Inorg. Chim. Acta*, 1983, **71**, 49.
27 T. K. Sham and G. M. Bancroft, *Inorg. Chem.*, 1975, **14**, 2281.
28 K. Kawakami and R. Okawara, *J. Organomet. Chem.*, 1966, **6**, 249.
29 T. N. Mitchell, *J. Organomet. Chem.*, 1973, **59**, 189.
30 G. Domazetis, R. J. Magee, and B. D. James, *J. Organomet. Chem.*, 1978, **148**, 339.
31 A. B. Crosby, R. J. Magee, and M. J. O'Connor, *Inorg. Chim. Acta*, 1979, **34**, 107.
32 P. J. Smith and L. Smith, *Inorg. Chim. Acta Rev.*, 1973, **7**, 11.
33 L. Vordonock and G. P. vander Kelen, *J. Organomet. Chem.*, 1972, **40**, 139.
34 J. Otera, T. Hinoishi, and R. Okawara, *J. Organomet. Chem.*, 1980, **202**, C93.
35 J. Otera, T. Hinoishi, Y. Kawabe, and R. Okawara, *Chem. Lett.*, 1981, 273.
36 A. G. Davies, P. G. Harrison, J. D. Kennedy, T. N. Mitchell, R. J. Puddephatt, and W. McFarlane, *J. Chem. Soc. C*, 1969, 1136.
37 W. McFarlane, J. C. Maire, and M. Delmas, *J. Chem. Soc., Dalton Trans.*, 1972, 1862.
38 H. C. Clark, V. K. Jain, I. J. McMahon, and R. C. Mehrotra, *J. Organomet. Chem.*, 1983, **243**, 299.
39 I. Douek, M. J. Frazer, Z. Goffer, M. Goldstein, B. Rimmer, and H. A. Willis, *Spectrochim. Acta, Part A*, 1967, **23**, 373.
40 L. Pauling, 'The Nature of the Chemical Bond,' 3rd edn., Cornell University Press, Ithaca, 1960, (*a*) p. 246; (*b*) p. 224; (*c*) p. 224, 229.
41 P. G. Harrison, T. J. King, and M. A. Healy, *J. Organomet. Chem.*, 1979, **182**, 17.
42 F. A. K. Nasser, M. B. Hossain, D. van der Helm, and J. J. Zuckerman, *Inorg. Chem.*, 1983, **22**, 3107.
43 I. A. Duncan and C. Glidewell, *J. Organomet. Chem.*, 1975, **97**, 51.
44 S. K. Saini, V. D. Gupta, and R. C. Mehrotra, *Aust. J. Chem.*, 1982, **35**, 2215.
45 D. K. Srivastava, V. K. Gupta, and V. D. Gupta, *Indian J. Chem.*, 1986, in the press; D. K. Srivastava, Anil K. Mishra, V. D. Gupta, and H. Nöth, unpublished work.
46 R. Beckett and B. F. Hoskins, *J. Chem. Soc., Dalton Trans.*, 1974, 622.
47 K. C. Molloy and J. J. Zuckerman, *Acc. Chem. Res.*, 1983, **16**, 386.

Received 8th January 1987; Paper 7/045